Autosomal Dominant MPAN : Mosaicism Expands the Clinical Spectrum to Atypical Late-Onset Phenotypes

Chloé Angelini, Christelle Marie Durand, Patricia Fergelot, Julie Deforges, Anne Vital, Patrice Menegon, Elizabeth Sarrazin, Rémi Bellance, Stéphane Mathis, Victoria Gonzalez, et al.

RESEARCH ARTICLE

Autosomal Dominant MPAN: Mosaicism Expands the Clinical Spectrum to Atypical Late-Onset Phenotypes

CME

Chloé Angelini, MD,[1,2,3] Christelle Marie Durand, PhD,[1,2,3,4] Patricia Fergelot, MD, PhD,[1,4] Julie Deforges, MLT,[1] Anne Vital, MD, PhD,[5] Patrice Menegon, MD,[6†] Elizabeth Sarrazin, MD,[7] Rémi Bellance, MD,[7] Stéphane Mathis, MD, PhD,[8] Victoria Gonzalez, MD, PhD,[9] Mathilde Renaud, MD, PhD,[10,11,12] Solène Frismand, MD,[10] Emmanuelle Schmitt, MD,[13] Marie Rouanet, MD,[14] Lydie Burglen, MD, PhD,[15] Brigitte Chabrol, MD, PhD,[16] Béatrice Desnous, MD, PhD,[16] Benoît Arveiler, PharmD, PhD,[1,4] Giovanni Stevanin, PhD,[3,17] Isabelle Coupry, PhD,[3,4*] and Cyril Goizet, MD, PhD[1,2,3,4]

[1]*Service de Génétique Médicale, Hôpital Pellegrin, CHU Bordeaux, Bordeaux, France*
[2]*Centre de Référence Maladies Rares «Neurogénétique», Service de Génétique Médicale, CHU Bordeaux, Bordeaux, France*
[3]*University of Bordeaux, CNRS, INCIA, UMR 5287, NRGen Team, Bordeaux, France*
[4]*MRGM, University of Bordeaux, INSERM U1211, Bordeaux, France*
[5]*Service d'Anatomie Pathologique, Hôpital Pellegrin, CHU Bordeaux, Bordeaux, France*
[6]*Service de Neuroradiologie, Hôpital Pellegrin, CHU Bordeaux, Bordeaux, France*
[7]*Centre de Référence Maladies Rares Neuromusculaires (AOC), Hôpital Pierre Zobda Quitman, CHU Martinique, Fort de France, Martinique*
[8]*Service de Neurologie (Unité Nerf-Muscle), Centre de Référence Maladies Rares, Neuromusculaires (AOC), Centre SLA, Hôpital Pellegrin, CHU Bordeaux, Bordeaux, France*
[9]*Service de neurologie, Hôpital Gui de Chauliac, CHU Montpellier, Montpellier, France*
[10]*Service de Neurologie, CHRU Nancy, Nancy, France*
[11]*Service de Génétique Clinique, CHRU Nancy, Nancy, France*
[12]*NGERE, INSERM U1256, Faculté de Médecine, Université de Lorraine, Nancy, France*
[13]*Service de Neuroradiologie Diagnostique et Thérapeutique, CHRU Nancy, Nancy, France*
[14]*Service d'explorations Fonctionnelles du Système Nerveux, Hôpital Pellegrin, CHU Bordeaux, Bordeaux, France*
[15]*Laboratoire de Neurogénétique Pédiatrique, Département de Génétique, Hôpital Trousseau, APHP.Sorbonne Université, Paris, France*
[16]*Service de Neuropédiatrie, Hôpital Timone enfants, APHM, Marseille, France*
[17]*EPHE, CNRS, INCIA, UMR 5287, PSL Research University, Paris, France*

ABSTRACT: Background: Mitochondrial membrane protein-associated neurodegeneration (MPAN) is caused by mutations in the *C19orf12* gene. MPAN typically appears in the first two decades of life and presents with progressive dystonia-parkinsonism, lower motor neuron signs, optic atrophy, and abnormal iron deposits predominantly in the basal ganglia. MPAN, initially considered as a strictly autosomal recessive disease (AR), turned out to be also dominantly inherited (AD).

Objectives: Our aim was to better characterize the clinical, molecular, and functional spectra associated with such dominant pathogenic heterozygous *C19orf12* variants.

Methods: We collected clinical, imaging, and molecular information of eight individuals from four AD-MPAN families and obtained brain neuropathology results for one. Functional studies, focused on energy and iron metabolism, were conducted on fibroblasts from AD-MPAN patients, AR-MPAN patients, and controls.

Results: We identified four heterozygous *C19orf12* variants in eight AD-MPAN patients. Two of them carrying the familial variant in mosaic displayed an atypical late-onset phenotype. Fibroblasts from AD-MPAN showed more severe alterations of iron storage metabolism and autophagy compared to AR-MPAN cells.

***Correspondence to:** Dr. Isabelle Coupry, Bordeaux University, INCIA CNRS UMR5287, NRGen Team, BBS Building, 2, Rue du Dr Hoffmann Martinot, 33076 Bordeaux Cedex, France; E-mail: isabelle.coupry@u-bordeaux.fr

Chloé Angelini, Christelle Marie Durand, Patricia Fergelot, Isabelle Coupry, and Cyril Goizet these authors contributed equally to this work.

[†]Deceased on March 22, 2022.

Relevant conflicts of interest/financial disclosures: Nothing to report.
Funding agency: This work was funded by the Agence de la BioMédecine (ClinicalTrials.gov, Identifier: NCT05615571).

Received: 8 February 2023; **Revised:** 31 May 2023; **Accepted:** 24 July 2023

Published online 21 August 2023 in Wiley Online Library (wileyonlinelibrary.com). DOI: 10.1002/mds.29576

Conclusion: Our data add strong evidence of the realness of AD-MPAN with identification of novel monoallelic *C19orf12* variants, including at the mosaic state. This has implications in diagnosis procedures. We also expand the phenotypic spectrum of MPAN to late onset atypical presentations. Finally, we demonstrate for the first time more drastic abnormalities of iron metabolism and autophagy in AD-MPAN than in AR-MPAN.

Key Words: NBIA; autosomal dominant MPAN; *C19orf12*; mosaicism; late-onset MPAN

Introduction

Neurodegeneration with brain iron accumulation (NBIA) represents an expanding group of rare inherited diseases characterized by progressive neurological features dominated by extrapyramidal movement disorders and abnormal iron deposits in the basal ganglia detected by brain magnetic resonance imaging (MRI).[1,2] Pathogenic variants in 10 genes are known to cause NBIA and at least five other genes are implicated in NBIA-like diseases.[3] Among those, *C19orf12* (HGNC symbol, *C19ORF12* MIM 614297) is implicated in autosomal recessive (AR) and dominant (AD) mitochondrial membrane protein-associated neurodegeneration (MPAN) (MIM 614298).[4,5] MPAN, also known as NBIA type 4, is most frequently recessively inherited (AR-MPAN) and is clinically characterized by dystonia, parkinsonism, spastic paraplegia, lower motor neuron signs, optic atrophy, behavioral troubles and cognitive decline. Age at onset is usually in the first two decades, but ranges from 4 to 30 years.[6] Brain MRI typically shows T2-weighted hypointensities in the globus pallidus (GP) and substantia nigra (SN). AD-MPAN is generally considered phenotypically indistinguishable from AR-MPAN although few cases have been reported up to now.[5-12]

The *C19orf12* gene, assigned to chromosome 19q, encodes a small transmembrane protein of unknown function localized in mitochondria, endoplasmic reticulum (ER) and mitochondria associated membranes (MAM).[4,13] Alternative transcripts are described combining 2 to 4 coding and/or non-coding exons. The major transcript, isoform 2 (NM_031448.6), is mainly expressed in adipose tissue and brain and encodes a predicted protein of 141 amino acids (15 kDa, UniProt KB). All the described AD-MPAN pathogenic variants are predicted truncating and are located in the last exon after amino acid 75 in the major transcript.[12] Although a dominant negative mechanism was first proposed,[5] a potential haploinsufficiency of the *C19orf12* isoform 3 (NM_001282929.1, NM_001282930.2, and NM_001282931.2) has been alternatively suggested to explain the molecular mechanisms involved in AD-MPAN.[12] The pathophysiological mechanisms leading to iron accumulation in MPAN are still elusive. A role of C19orf12 in lipid homeostasis, inhibition of apoptosis, and activation of autophagy has been proposed, altering mitochondrial functions and Ca^{2+} homeostasis when mutated.[4,13-15] Abnormal recycling of transferrin receptor (TfR1) and reduction of TfR1 palmitoylation have recently been proposed as a shared mechanism of iron overload among several NBIA, including MPAN.[16]

C19orf12 is a rather well conserved gene across species, allowing the recent development of two animal models expressing orthologs of *C19orf12*, namely drosophila and zebra-fish.[17,18] Down-regulation of the gene in both models has revealed alterations in brain development and locomotor behavior supporting the neurodegenerative phenotype observed in MPAN.

We report, here, eight additional AD-MPAN patients from four families identified by next generation sequencing (NGS). Among them, two unrelated patients displayed an atypical late-onset clinical presentation, with motoneuron involvement in one. Both were mosaic for the familial pathogenic variant. Functional studies were conducted on AD-MPAN patients' fibroblasts to investigate mitochondrial functions, autophagy and iron homeostasis.

Patients and Methods

Patients

The patients, here described, were gathered through the French reference diagnostic laboratory for NBIA (Bordeaux University Hospital) that offers genetic testing of NBIA, following routine diagnosis procedures. From 2012 to 2021, 184 patients were analyzed in the laboratory. Informed consent was obtained from each patient (including legal representatives for minor patients). Subsequently using a standardized questionnaire, family history, clinical, and MRI data were obtained from the referring clinicians. All procedures were carried out with adequate understanding and written consent signed by the patient, in accordance with the declaration of Helsinki and the French law. In addition, two siblings suffering from AR-MPAN followed at the department of genetics (Marseille, France) were also included in this study. All patients are defined in the text by their number as follow, P1 to P8 for AD-MPAN and P9 and P10 for AR-MPAN.

Neuropathology Analyses

Autopsy restricted to the brain was performed 12 hours after the patient death (family 2—patient 2). According to the GIE Neuro-CEB brain bank procedure (Economic Interest Grouping-Collection of Biological Samples for research on nervous system diseases), the right part of the brain was immersed in 10% formalin and frozen samples were collected from the left part. Preliminary examination was carried out on hematoxylin and eosin-stained paraffin sections, completed by Prussian blue staining and immunohistochemistry with antibodies against α-synuclein (Leica Biosystems, Nanterre, France), τ AT8 (Thermo Fisher Scientific, Bordeaux, France), β A4 amyloid (Dako, Agilent Technologies, Les Ulis, France), and prion protein 12F10 (Spibio, Interchim, Montluçon, France). The substrate-chromogen system was the 3,3′-diaminobenzidine (DAB) (Dako) for τ AT8, β A4 amyloid and prion protein. A high sensitivity 3-amino-9-ethylcarbazole (AEC) substrate-chromogen system (Dako) was used for α-synuclein staining.

Molecular Genetic Studies

Genomic DNA was extracted from total blood by Wizard genomic DNA Kit (Promega, Lyon, France) and from two frozen brain samples, one from the cortex, the other from basal ganglia, by DNA mini kit (Qiagen, Courtaboeuf, France). Molecular analysis of the four index patients was performed following our routine procedures by NGS of all coding exons and introns-exons junctions (−25/+25 bp) of *PANK2*, *PLA2G6*, *WDR45*, *C19orf12*, *FTL*, *FA2H*, *CP*, *DCAF17*, and *ATP13A2*. Sequencing details are described in the Supporting Data.

Search for *C19orf12* gene dosage anomaly was performed by semi quantitative multiplex fluorescent polymerase chain reaction (QMF-PCR). All primer sequences are available on request.

Functional Studies

Primary fibroblasts were obtained from arm skin biopsies from four patients (patients P3 and P5 from AD-MPAN cases, patients P9 and P10 who are AR-MPAN individuals) and three unrelated healthy controls matched in age and gender. Primary culture cells were grown as previously described.[19]

For western blotting, 3 to 30 µg of proteins were analyzed using conventional methods. A detailed description and the antibodies used are available in the Supporting Data.

Total iron contents were quantified with a ferrozine-based colorimetric iron assay,[20,21] with minor modifications. A detailed procedure is provided in Supporting Data.

Results

Clinical Description of the Cohort

All the AD-MPAN pedigrees are illustrated in Figure 1, and the main clinical and paraclinical data are presented in Table 1. Briefly, all patients displayed a typical MPAN phenotype, including walking difficulties and cognitive decline or intellectual disability, extrapyramidal features and spasticity were found in seven of them and four of eight cases showed ophthalmological abnormalities. All patients had abnormal brain MRI highly evocative of NBIA (Fig. 2 and Table 1). Typical MPAN-associated T2 and T2* hypointensity in the GP and the SN were present in all patients. A band of high signal intensity corresponding to internal medullary lamina was seen in the GP of five patients. Other MRI abnormalities were T2 hypointensity of the subthalamic nuclei in patient P3, frontotemporal cortical atrophy in patient P8, and diffuse cortical atrophy in patients P1 and P2.

Finally, six of eight patients had a classical MPAN disease course (ie, early age of onset and slow clinical progression).

The most striking observation concerned patients P2 and P4 who showed not only a much later age of onset (35 years), but also a very rapid disease time course leading to death in less than two decades. As detailed below, molecular analyses revealed the presence of a mosaic pathogenic variant in these two patients. In patient P2, the initial diagnosis since age 40 years was frontotemporal dementia (FTD) with motoneuron involvement. The correct diagnosis was established after he passed away, when AD-MPAN was diagnosed in his daughter (patient P3). The major clinical data of the mosaic patients are described below and full clinical information for all patients is provided in Supporting Data.

Clinical Description of Mosaic Patients

Patient P2—Family 2

The first symptoms appeared in middle 30s with apathy and behavioral troubles before developing aggressive and impulsive temper. Clinical examination at age 40 revealed extrapyramidal syndrome and a global reduced psychomotor activity. Brain MRI revealed T2 hypointensity in the GP, a discrete T2 hyperintense line in left GP suggestive of intern medullary lamina sign, and a diffuse cortical atrophy (Fig. 2A,B). At age 43, FTD was diagnosed based on the presence of sufficient diagnosis criteria (Table S1). Ophthalmological examination revealed a severe optic atrophy and excavation of the optical nerves. Muscle biopsy showed irregular fibers and neurogenic atrophy. The cerebral biopsy of the frontal lobes showed inflammation, but no sign of Alzheimer's disease nor Lewy bodies. Electrodiagnosis revealed reduced compound motor action potentials (CMAP) in the lower limbs

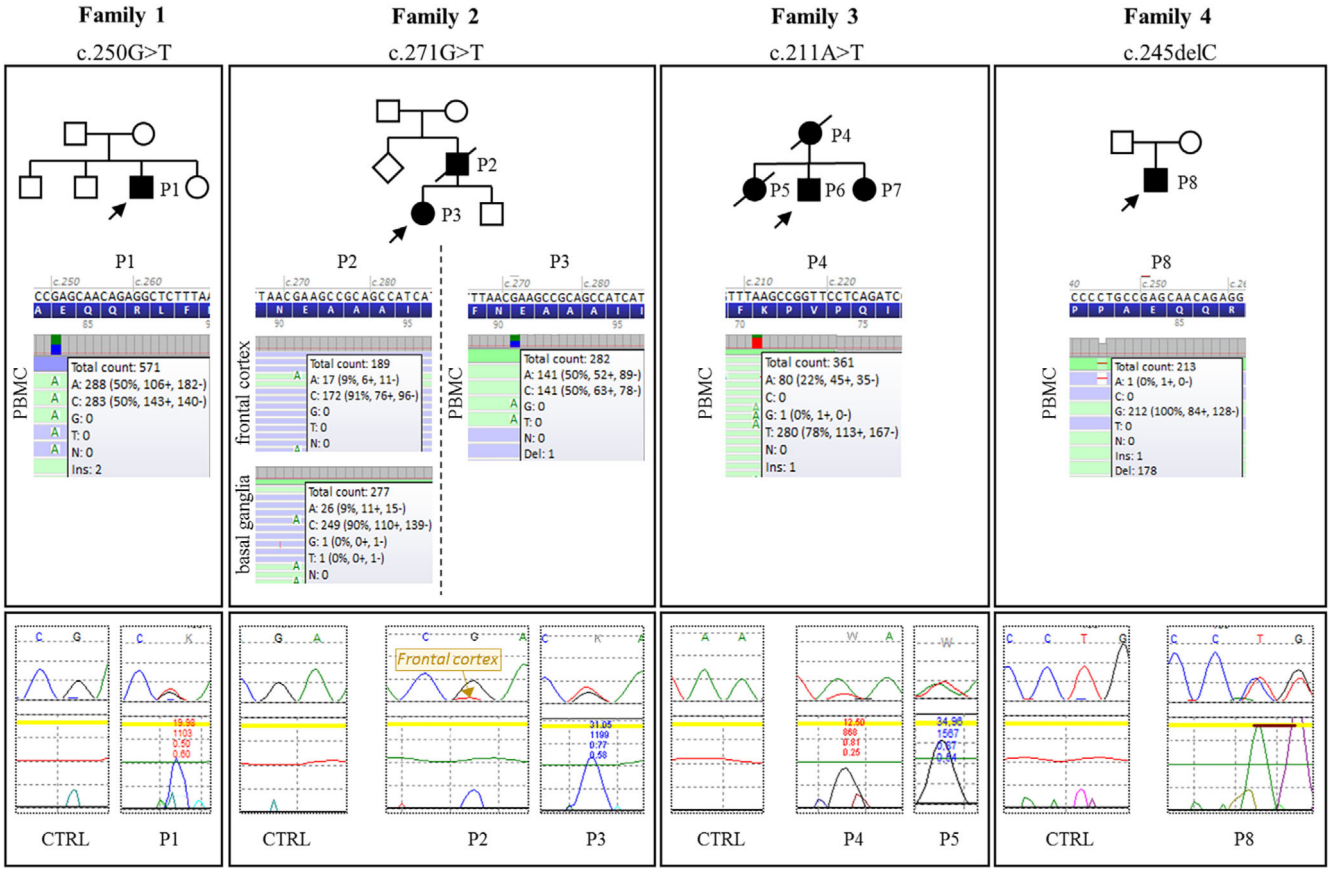

FIG. 1. Family pedigrees and molecular results (next generation sequencing [NGS] and Sanger sequencing data on electropherograms). Pedigrees (upper panel) and identification of *C19orf12* variants in probands and mosaic parents using NGS (medium panel) and Sanger sequencing (lower panels) in the four families. NGS reads are presented following a reverse complementary alignment on human genome (Hg19), showing the wild-type nucleotide as a T (patients P4 and P5) or a C (patients P2 and P3) and the variant as an A (Interface from Alamut visual Software). For patients P2 and P4 mosaïcism was calculated as 2-fold the percentage of variant nucleotides considering at these positions in total reads a 50% proportion of each allele, as shown for patient P3. In lower panels, electropherograms of forward Sanger sequencing display *C19ORF12* coding DNA (Mutation Surveyor software). Of note the barely visible mosaic variant c.271G > T in frontal cortex of patient P2 with the Sanger method (P2, see arrow). [Color figure can be viewed at wileyonlinelibrary.com]

(LL) Needle electromyography showed reduced recruitment pattern with polyphasic aspect and large amplitude of motor unit potentials, mainly in the LL, suggestive of a chronic motor neuron disorder. Symptoms slowly worsened, indeed he became bed-ridden at age 44 and died at age 52 years. Post mortem brain examination was performed.

Patient P4—Family 3

This 44-year-old-woman was known since childhood to have mild intellectual deficiency of undetermined cause associated with short height and microcephaly. Clear walking difficulties, which rapidly worsened, and severe cognitive deficit were noted at age 39. Examination showed severe spasticity and moderate muscle weakness of the four limbs predominant on LL. Brain MRI showed bilateral GP T2* hypointensities and moderate T2 hypointensities in SN, associated to a major cortical and sub cortical atrophy (Fig. 2G). A discrete T2 hyperintense line in the right GP may suggest the sign of the intern medullary lamina. She used a walker at age 39 and a wheelchair at age 40. Ability to talk was lost at age 42. She was bedridden at age 44 and died at age 47.

Molecular Genetics

In the four studied families, the molecular analyses revealed four different truncating variants located in the 3rd (last) exon of *C19orf12* (MANE select NM_031448.6; NP_113636.2): three nonsense c.250G > T, p.(Glu84*), c.271G > T, p.(Glu91*), c.211A > T, p.(Lys71*), and one frameshift variant c.245delC, p.(Pro82Leufs*26) (Fig. 1). The first two non-sense variants had never been described, unlike the two other variants.[5,9,12] They were all absent from gnomAD database (v2.1.1, 2022.11.26) and classified as pathogenic according to American College of Medical Genetics and Genomics/American Association of Molecular Pathology guidelines (PVS1-VSTR, PM2-MOD, and PP1-SUP).[22] It was not possible to check a de novo occurrence in the two sporadic cases born from non-consanguineous healthy parents (P1 and P8). In

TABLE 1 *Clinical and paraclinical data of the AD-MPAN patients*

Patients	P1	P2	P3	P4	P5	P6	P7	P8
Family history	−	+	+	+	+	+	+	−
Age at onset (years)	Childhood	35	8	35	6	10	6	25
Signs at onset	Clumsiness, walking difficulties	Behavioral troubles	Learning and walking difficulties	Walking difficulties	Walking difficulties	Walking difficulties	Learning difficulties	Dementia
Age at last examination (years)	31	43	28	44	25	23	17	28
ID since childhood	Yes	No	No	No	No	Yes	Yes	No
Dystonia	+	ND	ND	+	ND	ND	−	+
Akinesia/ hypokinesia-rigidity	+	+	+	+	+	+	−	+
Chorea	−	−	+	+	−	−	−	−
Pyramidal syndrome	+	+	+	+	+	+	−	+
Ataxia	ND	ND	+	ND	−	+	+	−
Muscle weakness and atrophy	ND	ND	+	+	+	+	−	−
Loss of walking	27	ND	26	43	10	24	−	ND
Epilepsy	+	+	−	−	−	−	−	−
Cognitive decline	+	+	+	+	+	+	−	+
Psychiatric symptoms	Acute psychotic episode	Depression	Depression	−	−	−	−	+
Apathy	ND	+	+	+	−	+	−	+
Eye fundus	Normal	Optic atrophy	Optic atrophy	ND	Retinal degeneration	Age 17 Normal	Age 14 Retinal degeneration	ND

(Continues)

TABLE 1 *Continued*

Patients	P1	P2	P3	P4	P5	P6	P7	P8
EMNG	ND	Motor neuropathy	Motor neuropathy	ND	ND	ND	ND	ND
Brain MRI findings	Age 24 Deposits on basal ganglia, mostly on GP and putamen, severe cerebral diffuse atrophy	Age 41 Diffuse atrophy, deposits on GP. Suspicion of IML sign on left GP	Age 19 and 22 Deposits on basal ganglia, mostly on GP and SN. IML sign on right GP	Age 39 HypoT2 and T2⋆ GP and SN. Suspicion of IML sign on right GP Moderate cerebellar atrophy Cortical and sub-cortical atrophy	Age 25 HypoT2 and T2⋆ GP and SN. Bilateral IML sign. Moderate cerebellar atrophy Cortical and sub-cortical atrophy	Age 23 HypoT2 and T2⋆ GP and SN Bilateral IML sign. Cortical and sub-cortical atrophy	Age 18 HypoT2 in GP and SN, and more subdued hypoT2 in red nuclei	Age 27 Global deposits on basal ganglia (SWI hypointensities) and frontotemporal atrophy
Age at death (years)	ND	52	NA	47	28	NA	NA	NA
Pathogenic variant	c.250G > T, p.(Glu84⋆)	c.271G > T, p.(Glu91⋆)	c.271G > T, p.(Glu91⋆)	c.211A > T, p.(Lys71⋆)[9]	c.211A > T, p.(Lys71⋆)[9]	c.211A > T, p.(Lys71⋆)[9]	c.211A > T, p.(Lys71⋆)[9]	c.245del, p.(Pro82Leufs⋆26)[5,12]
Mosaïcism	–	+, 20% in brain	–	+, 44% in blood	–	–	–	–
Variant in gnomAD	–	–	–	–	–	–	–	–

Note: The grey shade highlights the 2 patients with late-onset phenotype and variant mosaicism.
Abbreviations: AD-MPAN, autosomal dominant mitochondrial membrane protein-associated neurodegeneration; +, present; −, absent; ND, no data; MRI, magnetic resonance imaging; GP, globus pallidus; IML, intern medullary lamina; SN, substantia nigra; SWI, susceptibility weighted imaging; NA, not adapted.

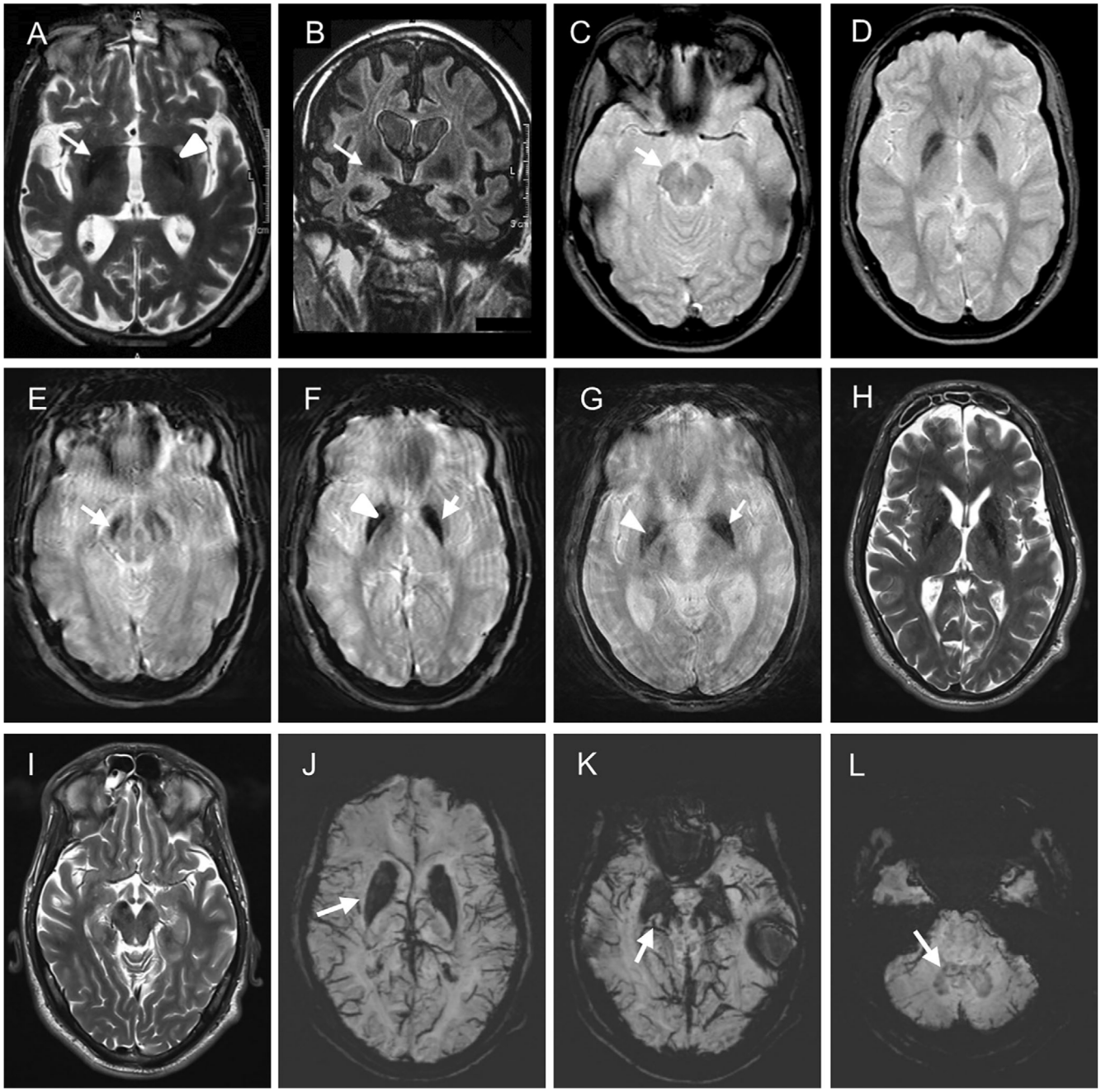

FIG. 2. Brain magnetic resonance imaging. (**A,B**) Patient P2, axial T2-weighted imaging with hypointensity on globus pallidus (**A**) with discrete linear hyperintensity in left globus pallidus, suggesting intern medullary lamina sign (arrowhead). In (**B**) coronal fluid attenuated inversion recovery-weighted imaging with hypointensity on globus pallidus (white arrow) and cortical atrophy. (**C-F**) Patient P3 at 18 years (**C,D**) and 23 years (**E,F**). We observed a worsening of iron deposits on globus pallidus, red nuclei, and substantia nigra. Hypointensity in T2* or susceptibility weighted imaging (SWI) (white arrows) suggest iron deposits. In (**F**) linear hyperintensity in right globus pallidus (arrowhead) underlines the intern medullary lamina sign. (**G**) Patient P4, axial T2* weighted imaging with hypointensity on globus pallidus (white arrow), and suspicion of intern medullary lamina sign on right globus pallidus (arrowhead). (**H,I**) Patient P8, axial T2-weighted imaging with hypointensity on globus pallidus and putamen, red nuclei and substantia nigra; (**J-L**) Patient P8, axial mIP SWI (minimum Intensity Projection) with hypointensity on putamen, red nuclei, and dentatus nuclei.

families 2 and 3, the variants segregated with the disease, and somatic mosaicism was identified in both affected parents, patients P2 and P4 (Fig. 1). Of note for patient P2, despite a massive parallel sequencing (>100X) the variant was not called when applying the software low stringency filters therefore, requiring a lower calling threshold (variant allele frequency <10%) to be automatically retrieved in the variant calling file (.vcf), closer to the limit of detection.

Interstitial deletions and large rearrangements have been excluded by QMF-PCR (patients P1, P3, P6, and P8).

The AR-MPAN patients P9 and P10, used in cellular experiments, were compound heterozygous for c.105delA, p.(Ala37Profs*25), and c.383A > G, p.(Tyr128Cys) both absent from gnomAD, and the missense variant has already been described in trans with another truncating variant.[9]

Neuropathological Findings

The fresh brain of patient P2 weighed 1000 g and was atrophic. After formalin fixation, coronal sections of the right cerebral hemisphere and horizontal sections of the brain stem showed a marked pallor of the SN and locus coeruleus. Microscopic examination of frontal, temporal, and occipital cortical areas revealed marked neuronal loss with a spongiform pattern (Fig. 3A). Similar, but less severe lesions were observed in the amygdala, entorhinal cortex, and hippocampus. Neuronal depletion, Lewy bodies, and axonal spheroids were observed in the putamen, GP, caudate nucleus, thalamus, SN (Fig. 3B), locus coeruleus, and dorsal nucleus of the vagus. Prussian blue staining of protein-bound ferric iron identified minimal iron deposition limited to the globus pallidus. Immunohistochemistry with anti-α synuclein confirmed the presence of Lewy bodies and Lewy neurites in the sub-cited areas (Fig. 3C,D), but also revealed α-synuclein aggregates in cortical neurons and pyramidal neurons of hippocampus (Fig. 3E). Anti-τ AT8 revealed hyperphosphorylated τ-containing neurons, which were numerous in

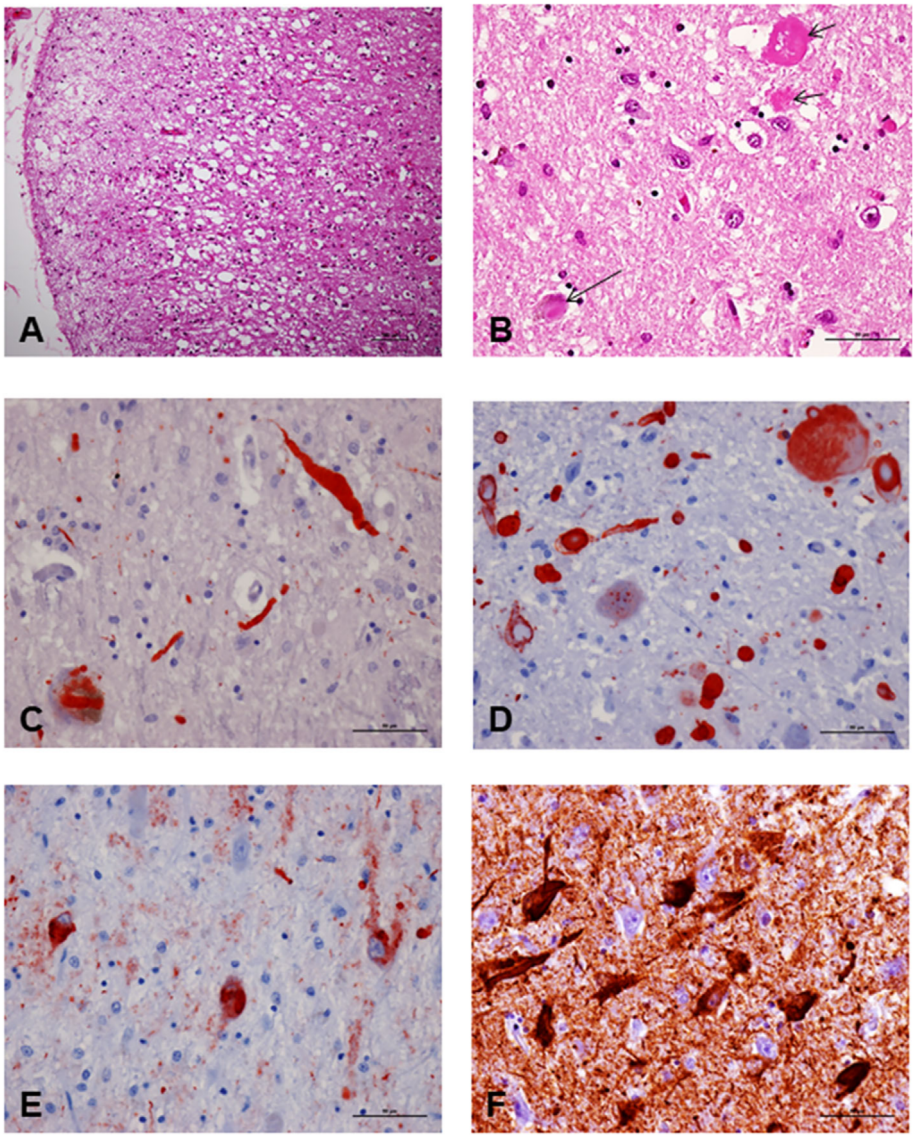

FIG. 3. Histopathology on paraffin section, brain of patient P2. Hematoxylin and eosin staining showing neuronal loss with a spongiform pattern in the frontal cortex (**A**), an intra-neuronal Lewy body (long arrow) and two axonal spheroids (short arrows) in the substantia nigra (**B**). Anti-α synuclein immunohistochemistry showing Lewy bodies and Lewy neurites in the locus ceruleus (**C**) and the dorsal nucleus of the vagus (**D**); α-synuclein aggregates are also present in pyramidal neurons of the hippocampus (**E**). Anti-τ AT8 immunohistochemistry showing hyperphosphorylated tau-containing pyramidal cells in the hippocampus (**F**). Bar = 100 μm in (**A**). Bar = 50 μm in (**B**)-(**F**). [Color figure can be viewed at wileyonlinelibrary.com]

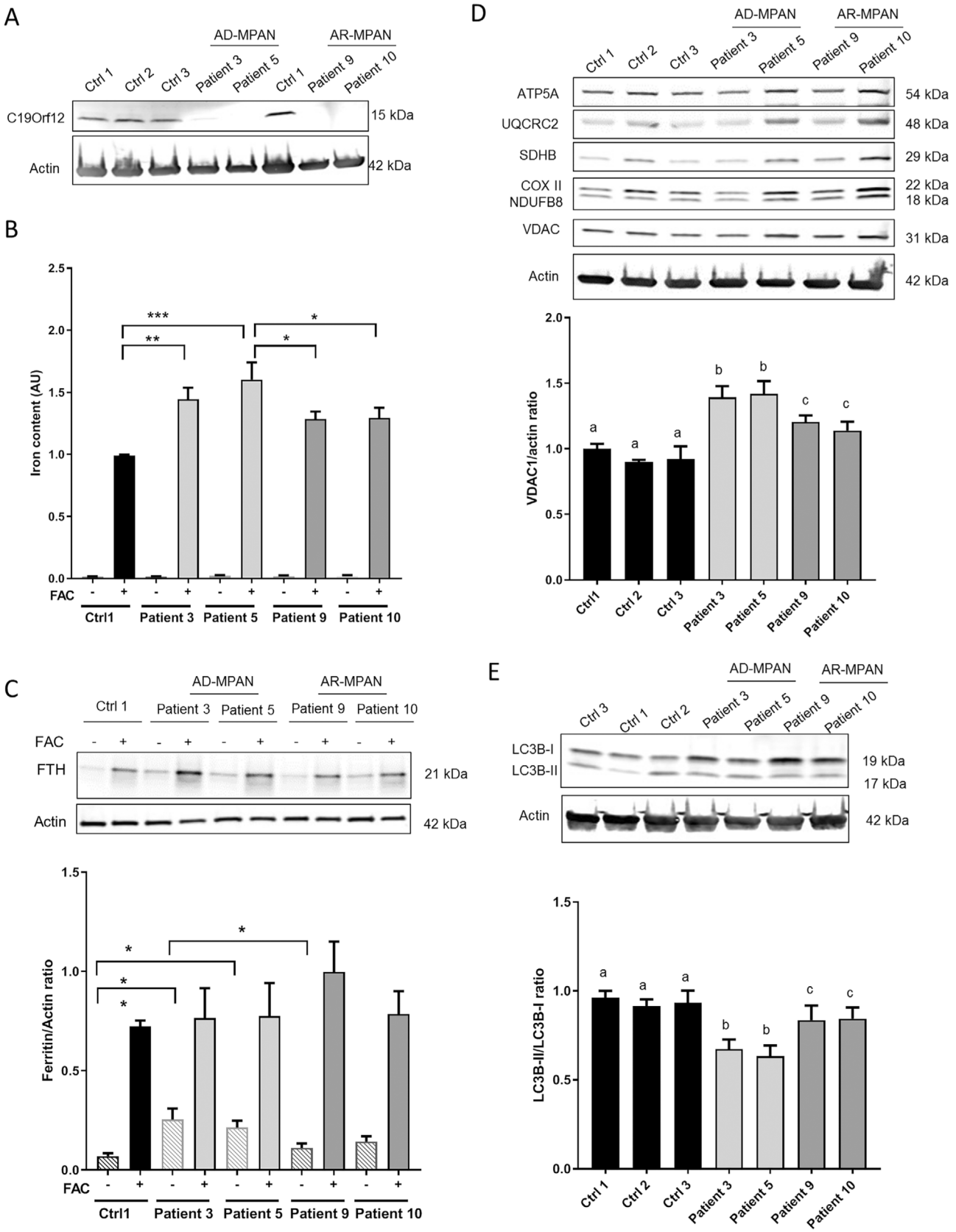

FIG. 4. Legend on next page.

hippocampus (Fig. 3F) and few in cortical areas. No specific deposit was identified with antibodies against β A4 and prion proteins.

Functional Studies

Expression of C19orf12 in Patients' Fibroblasts

Western blot analysis revealed the endogenous C19orf12 protein in control fibroblasts as a band of 15 kDa at the predicted size (Fig. 4A). Indeed, this band was absent in AR-MPAN cells and barely detectable in AD-MPAN cells.

The very low level of C19orf12 detection in AD-MPAN cells is unlikely because of low levels of transcripts, which were not significantly different between patients and controls (data not shown).

Abnormal Iron Homeostasis Was Observed in AD-MPAN

Total iron content was quantified in cultured fibroblasts using a ferrozine-based colorimetric assay and compared between AD-, AR-MPAN, and one control.[20,21] In low iron conditions (−FAC), iron was similarly undetectable in all fibroblasts. As expected, iron incubation (+FAC) led to a major increase of intracellular iron in all cells compared to non-treated cells (−FAC). Interestingly, treated AD-MPAN cells exhibited a significant increase in iron content with an average change of 1.5-fold compared to control cells ($P < 0.01$ and $P < 0.001$) (Fig. 4B), whereas AR-MPAN cells showed a non-significant 1.2-fold change when compared to the control. These data highlight abnormal iron accumulation in AD-MPAN and only a trend to overload in AR-MPAN.

Ferritin is the major intracellular iron storage protein complex, including ferritin light polypeptide (FTL) and ferritin heavy polypeptide (FTH). We investigated by western blot the level of FTH in fibroblasts with (+FAC) or without iron treatment (−FAC) (Fig. 4C). In –FAC condition, AD-MPAN cells exhibited the highest FTH expression with a significant 3.6-fold increase versus control cells ($P < 0.05$ and $P < 0.01$) (Fig. 4C). In AR-MPAN cells, this mean fold change was only 1.8 (not significant). In +FAC condition, the same magnitude in FTH increase was observed in all treated cells.

Therefore, when comparing AD-MPAN to AR-MPAN and control cells, our data suggest a proportionate response to iron loading in both forms.

An Increased Amount of Mitochondria Was Detected in AD-MPAN

C19orf12 has been localized both in mitochondria and ER[4,23] and MPAN patient's fibroblasts showed mitochondrial dysfunction.[13-15]

Therefore, we investigated by western blot analysis of fibroblast lysates the effect of *C19orf12* variants on the steady-state levels of mitochondrial proteins, for instance, individual OXPHOS complex subunits and the outer membrane protein VDAC1 (Fig. 4D).

The sole significant change versus control was a mild increase of VDAC1 observed only in AD-MPAN cells (1.4 mean fold change), suggesting an increased amount of mitochondria in these cells. Once again, a milder effect was observed in the AR-MPAN cells. We hypothesized that the increased expression of VDAC1 could result from higher mitochondria biogenesis and/or a defect in mitophagy, a selective pathway of autophagy.

Alteration of Autophagy

LC3B-I (heavy form) is transformed into LC3B-II (light form) when autophagy is effective either constitutively or under various stimuli. Keeping standard culture conditions, we observed a lower LC3B-II /LC3B-I ratio in AD-MPAN than in control cells, although this ratio was unchanged in AR-MPAN cells (Fig. 4E), suggesting that autophagy is defective in AD-MPAN cells.

Discussion

Until recently the inheritance of *C19orf12* pathogenic variants was thought to be strictly autosomal recessive.[11,24] However, several recent reports paved the way for parallel existence of a dominant form (Table S2).[5-12,15,25] To date, among the 18 monoallelic candidate variants reported in

FIG. 4. Functional studies in patients' fibroblasts. (**A**) Representative immunoblot of C19orf12 expression using anti-C19orf12 and anti-β-actin antibodies on proteins extracted from patients and controls cells (n = 4). (**B**) Iron quantification using the ferrozine-based colorimetric assay in fibroblasts from 4 patients and 1 control in fetal bovine serum-free Dulbecco's Modified Eagle Medium with low iron (−FAC) or high iron (+FAC) conditions. Data are expressed as mean ± standard error of the mean (SEM) of independent experiments (n = 7–9). ***$P < 0.001$; **$P < 0.01$; *$P < 0.05$. (**C**) Representative immunoblot of ferritin expression using anti-ferritin (H + L) and anti-β-actin antibodies on proteins extracted from patients and controls cells. Quantification of H-Ferritin (FTH) relative to β actin. Data are expressed as mean ± SEM of independent experiments (n = 6–8); **$P < 0.01$; *$P < 0.05$. (**D**) Western blot analyses of mitochondrial OXPHOS respiratory proteins ATP synthase 5A (Complex V, 54 kDa), COX II (complex IV, 22 kDa), UQCRC2 (complex III, 48 kDa), SDHB (complex II, 29 kDa), and NDUFB8 (complex I, 18 kDa), VDAC1, and actin in patients' cells compared to control samples. Quantification of VDAC1 relative to β actin. Data normalized to Ctrl1 are expressed as mean ± SEM of independent experiments (n = 6–8), group "b" is significantly different from group "a", group "c" is not significantly different from group "a" and group "b." (**E**) Representative immunoblot using anti-LC3B (autophagy marker) and anti-β actin antibodies on proteins extracted from patients and controls cells. Quantification of LC3B-II to LC3B-I ratio. Data normalized to Ctrl1 are expressed as mean ± SEM of independent experiments (n = 5–7), group "b" is significantly different from group "a", group "c" is not significantly different from group "a" and group "b". Groups that are not significantly different at $P < 0.01$ are indicated by the same letter. AD-MPAN, autosomal dominant MPAN; AR-MPAN, autosomal recessive MPAN; Ctrl, control; MPAN, mitochondrial membrane protein-associated neurodegeneration.

22 unrelated AD-MPAN families,[11,12] only nine variants are supported by strong evidences of pathogenicity: six identified in sporadic cases,[5,8,1,2,5] and three in families.[5,10] Additional eight sporadic cases with unavailable parental DNA were described.[5] In the other patients carrying a heterozygous variant, a second hidden variant in *C19orf12* or the involvement of another yet unknown NBIA gene has been suspected.[5,8]

Our study corroborates these evidences and adds four variants, two of which are novel, identified in eight patients with AD-MPAN. We cannot exclude a de novo occurrence of the variants found in the two sporadic cases as parental DNAs were unavailable. In familial presentations (families 2 and 3), the variant co-segregated with the disease. More importantly, the affected parent (patients P2 and P4) corresponding to the first generation affected in both families, was in fact carrying the familial variant at a mosaic state, indicating a post-zygotic mutational event. Therefore, the identification in affected children of a homogeneous *C19orf12* variant transmitted by a mosaic parent suffering from neurodegeneration clearly proved the dominant mode of transmission of MPAN in both families.

Very interestingly, these two AD-MPAN patients carrying a mosaic *C19orf12* pathogenic variant (patients P2 and P4) started their disease during their 30s, much later in life than their affected offspring as well as than previously described AR-MPAN and AD-MPAN patients. We had access to brain DNA from the cerebral cortex and basal ganglia from patient P2, allowing us to identify for the first time a very low level of mosaicism in both structures. Very importantly, this patient had received an erroneous diagnosis of frontotemporal dementia according to the consensus criteria in 1998 (FTD criteria in Table S1) with motoneuron involvement at the age of 43 and has been followed for this condition by neurologists until his death.[26] Description of this particular clinical presentation in our series, with late-onset inaugural behavioral symptoms, is crucial for genetic counseling. Indeed, in these two families, the index cases who presented a typical form of MPAN (patients P3 and P6) were offspring of mosaic individuals, for whom diagnosis of AD-MPAN was much delayed. It is, therefore, crucial to trace the family history and to search for the pathogenic variant of *C19orf12* in the two parents of children diagnosed with MPAN. Facing an early presentation of cognitive decline mimicking FTD, the diagnosis of mosaic *C19orf12* should be evoked, and therefore, be investigated at the molecular level using a more sensitive computational screening tool than standard NGS variant calling pipelines.[27]

Although the existence of two modes of inheritance, recessive and dominant, appears now irrefutable in MPAN, no clinical differences were previously reported between them.[5,11] Our series of eight AD-MPAN patients strongly argues for this, excepted for patients with mosaicism who display later onset.

The MRIs of the different patients allow the temporality of the iron deposits to be traced. At the supratentorial level, the globi pallidi are the first to be affected, followed by the putamen and the caudate nuclei, with cortical atrophy appearing later, predominantly in the frontotemporal region. There is no eye of tiger sign, but the typical intern medullary lamina sign is found in five patients of our series, therefore, questioning the true existence of the eye of the tiger sign in MPAN. On re-reading the MRIs of MPAN patients described in the literature, it appears that the hyperintensities described as an eye of the tiger sign are generally intern medullary lamina sign.[28-30] In the infratentorial region, the involvement is predominant in the SN and to a lesser extent in the red nuclei. The MRI pattern of iron deposits in AD-MPAN is, therefore, similar to AR-MPAN.[6]

Neuropathological studies in MPAN patients have been occasionally reported. Two of them were affected by AD-MPAN, with an onset in adulthood and an evolution leading to death within 10 years for one and 30 years for the other.[5] Two other individuals had AR-MPAN, with onset in childhood for one of the patients[4] and in adulthood for the other.[6] Our data are consistent with the literature and confirm similarities between dominant and recessive MPAN patients. Iron deposits are found predominantly in the GP, as well as axonal spheroids and Lewy bodies, and more discretely phosphorylated τ protein labeling, primarily in the hippocampus. However, no neurofibrillary tangles or amyloid plaques were found. In NBIA, the presence of Lewy bodies is not unique to MPAN, but is also found in almost all patients with PLA2G6-associated neurodegeneration (PLAN).[31] Patients P2 and P4 are the only demonstrated mosaic cases reported to date. Without genetic testing of another tissue like blood or fibroblasts in patient P2, one cannot rule out the possibility that the brain mutated cells constitute the prominent fraction of neuronal loss, therefore, contributing to the detection of a very low fraction of heterozygosity and a minimal residual iron deposition in the GP. Strikingly, despite the low to moderate level of mosaicism in the brain, patient P2 has major neuropathological impairment similar to the classical forms, regardless of the inheritance mode, with the same time course once the symptoms appear.

The four *C19orf12* variants described here in the last exon, three nonsense and one frameshift, were truncating after amino acid 71 with positions similar to those previously described in the literature.[5,8,12] Gregory et al[5] first proposed a dominant-negative mechanism for AD-MPAN, by which the truncated protein would multimerize with the wild-type protein, resulting in a loss of function. This mechanism could explain the lack of phenotypic difference between AD-MPAN and AR-MPAN. It was also suggested that the mechanism of pathogenicity may be related to the isoform impacted by the variant. Because of their exclusive location in the last exon of

C19orf12, the truncating variants described in AD-MPAN would ultimately be loss-of-function variants.[12] In control fibroblasts, we detected the expression of the endogenous protein C19orf12 at the predicted size of 15 kDa. For the first time, we could observe a residual protein in the fibroblasts of proven AD-MPAN patients. Therefore, a strong decrease in C19orf12 expression leads at least to a partial loss of function without prejudging the underlying mechanism (ie, dominant-negative effect or haploinsufficiency).

The observation of a more pronounced cellular phenotype of AD-MPAN versus AR-MPAN remains unexplained. Taking into account that the precise function of C19orf12 is still unknown, due in part to the persistent imperfect knowledge of the structure and cellular location of the different isoforms, the functional effects demonstrated here, and by others, are most likely surrogate markers. Therefore, other relevant aspects of MPAN pathophysiology could be ignored as the protein function is not directly addressed. Further studies are necessary to elucidate the mechanisms by which the different heterozygous variants of C19orf12 cause cellular damages.

Iron accumulation was observed in MPAN patients, but how this accumulation led to neurodegeneration remains elusive.[14,16] Here, AD-MPAN fibroblasts incubated in iron-rich medium, displayed a significantly higher iron accumulation than the healthy control cells. Nevertheless, given their higher basal level of ferritin, the response of AD-mutated cells may be considered maladaptive, suggesting a dysregulation of iron storage. These abnormalities of iron content are not specific to MPAN, but are found in other subtypes of NBIA and also in Friedreich's ataxia.[32] It was suggested that these abnormalities are related to a defect in TfR1 palmitoylation, leading to a defective recycling, thereby increasing iron entry into the cell through the transferrin-dependent pathway.[16] Our results in AD patient's cells point out a possible impairment of ferritin turnover with a delayed iron-related, fine-tuned regulation of its synthesis that could rely on a decreased sensitivity of sensors like iron regulatory protein/iron-responsive element (IRP2/IRE) and/or of altered ferritinophagy. How a paradoxically higher level of ferritin in low iron conditions, namely in AD-MPAN FAC-cells, results from C19orf12 loss of function remains poorly understood and need further insights. This may also reflect protection against toxicity of pre-existing iron overload in these cells. Indeed, ferritin elevation after iron loading in FAC+, AD-MPAN cells is lower than that in wild-type and AR-MPAN cells suggesting impaired homeostasis.

Finally, reminiscent of previous observations in C19orf12 overexpressing cells,[13] an inverse variation of LC3B ratio in AD-MPAN cells also suggest an alteration of autophagy, as recently shown.[15] Such impairment is thought to play a role in two other NBIA subtypes, β-propeller protein-associated neurodegeneration (BPAN) and Kufor-Rakeb syndrome, of which causative genes are *WDR45* and *ATP13A2*, respectively.[33] Taken together, our data and overexpression studies suggest a possible role of *C19orf12* in controlling selective autophagy (ie, mitophagy and ferritinophagy). In fact, several different pathways could contribute to intracerebral iron accumulation through cumulative effect of increased iron entry and altered autophagy. Further studies exploring the interplays between mitophagy, ferritinophagy, and the cellular pathways of iron metabolism are needed to precise the role of *C19orf12* in ferroptosis, an iron-induced cell death.[13,14]

In conclusion, the description of these eight patients strongly complements knowledge about AD-MPAN. The possibility of late-onset presentations, mimicking frontotemporal dementia and motor neuron involvement, in association with somatic mosaicism is crucial information for genetic counseling in AD-MPAN families. The precise mechanism leading to cellular iron accumulation remains an open question, as does the iron deposits temporality, brain MRI lesions visibility and their link to the clinical symptoms, onset, and course, in AD-MPAN and other NBIAs. Improving our knowledge on NBIA genes function is the main challenge in the coming years. The aim is to clarify the early pathogenic steps leading to excessive iron storage and to determine how they could be targeted to slow down the progression of the disease, by limiting iron accumulation and preventing cellular damages.

Acknowledgments: This work was funded by the Agence de la biomédecine (ClinicalTrials.gov, Identifier: NCT05615571). We are grateful to the patients and their families for participating in this project, as well as to the International Foundation for Research in Alzheimer Disease (Ifrad), and the GIE Neuro-CEB who provided brain samples from patient P2.

Ethics Statement

All study sites obtained ethics approval from local institutional review boards and complied with all applicable national, ethics, and regulatory guidelines. The study was conducted according to the guidelines of Good Clinical Practice and is in full compliance with the Declaration of Helsinki and its 2013 amendment. Informed consent or assent was obtained from all participants as required by the institutional review boards.

Data Availability Statement

The data that support the findings of this study are available on request from the corresponding author. The data are not publicly available owing to privacy or ethical restrictions.

References

1. Hogarth P. Neurodegeneration with brain iron accumulation: diagnosis and management. J Mov Disord 2015;8(1):1–13. https://doi.org/10.14802/jmd.14034
2. Hayflick SJ, Kurian MA, Hogarth P. Chapter 19 - neurodegeneration with brain iron accumulation. In: Geschwind DH, Paulson HL, Klein C, eds. Handbook of Clinical Neurology. Vol 147. Neurogenetics, Part I. London: Elsevier; 2018:293–305. https://doi.org/10.1016/B978-0-444-63233-3.00019-1.
3. Lehéricy S, Roze E, Goizet C, Mochel F. MRI of neurodegeneration with brain iron accumulation. Curr Opin Neurol 2020;33(4):462–473. https://doi.org/10.1097/WCO.0000000000000844
4. Hartig MB, Iuso A, Haack T, et al. Absence of an orphan mitochondrial protein, C19orf12, causes a distinct clinical subtype of neurodegeneration with brain iron accumulation. Am J Hum Genet 2011;89(4):543–550. https://doi.org/10.1016/j.ajhg.2011.09.007
5. Gregory A, Lotia M, Jeong SY, et al. Autosomal dominant mitochondrial membrane protein-associated neurodegeneration (MPAN). Mol Genet Genomic Med 2019;7(7):e00736. https://doi.org/10.1002/mgg3.736
6. Hogarth P, Gregory A, Kruer MC, et al. New NBIA subtype: genetic, clinical, pathologic, and radiographic features of MPAN. Neurology 2013;80(3):268–275. https://doi.org/10.1212/WNL.0b013e31827e07be
7. Panteghini C, Zorzi G, Venco P, et al. C19orf12 and FA2H mutations are rare in Italian patients with neurodegeneration with brain iron accumulation. Semin Pediatr Neurol 2012;19(2):75–81. https://doi.org/10.1016/j.spen.2012.03.006
8. Monfrini E, Melzi V, Buongarzone G, et al. A de novo C19orf12 heterozygous mutation in a patient with MPAN. Parkinsonism Relat Disord 2018;48:109–111. https://doi.org/10.1016/j.parkreldis.2017.12.025
9. Gagliardi M, Annesi G, Lesca G, et al. C19orf12 gene mutations in patients with neurodegeneration with brain iron accumulation. Parkinsonism Relat Disord 2015;21(7):813–816. https://doi.org/10.1016/j.parkreldis.2015.04.009
10. Balicza P, Bencsik R, Lengyel A, et al. Novel dominant MPAN family with a complex genetic architecture as a basis for phenotypic variability. Neurol Genet 2020;6(5):e515. https://doi.org/10.1212/NXG.0000000000000515
11. Fraser S, Koenig M, Farach L, Mancias P, Mowrey K. A De Novo case of autosomal dominant mitochondrial membrane protein-associated neurodegeneration. Mol Genet Genomic Med 2021;9(7):e1706. https://doi.org/10.1002/mgg3.1706
12. Rickman OJ, Salter CG, Gunning AC, et al. Dominant mitochondrial membrane protein-associated neurodegeneration (MPAN) variants cluster within a specific C19orf12 isoform. Parkinsonism Relat Disord 2021;82:84–86. https://doi.org/10.1016/j.parkreldis.2020.10.041
13. Venco P, Bonora M, Giorgi C, et al. Mutations of C19orf12, coding for a transmembrane glycine zipper containing mitochondrial protein, cause mis-localization of the protein, inability to respond to oxidative stress and increased mitochondrial Ca2+. Front Genet 2015;6:185. https://doi.org/10.3389/fgene.2015.00185
14. Shao C, Zhu J, Ma X, et al. C19orf12 ablation causes ferroptosis in mitochondrial membrane protein-associated with neurodegeneration. Free Radic Biol Med 2022;182:23–33. https://doi.org/10.1016/j.freeradbiomed.2022.02.006
15. Zanuttigh E, Derderian K, Güra MA, et al. Identification of autophagy as a functional target suitable for the pharmacological treatment of mitochondrial membrane protein-associated neurodegeneration (MPAN) in vitro. Pharmaceutics 2023;15(1):267. https://doi.org/10.3390/pharmaceutics15010267
16. Drecourt A, Babdor J, Dussiot M, et al. Impaired transferrin receptor Palmitoylation and recycling in neurodegeneration with brain iron accumulation. Am J Hum Genet 2018;102(2):266–277. https://doi.org/10.1016/j.ajhg.2018.01.003
17. Iuso A, Sibon OCM, Gorza M, et al. Impairment of Drosophila orthologs of the human orphan protein C19orf12 induces bang sensitivity and neurodegeneration. PloS One 2014;9(2):e89439. https://doi.org/10.1371/journal.pone.0089439
18. Mignani L, Zizioli D, Borsani G, Monti E, Finazzi D. The down-regulation of c19orf12 negatively affects neuronal and musculature development in zebrafish embryos. Front Cell Dev Biol 2020;8:596069. https://doi.org/10.3389/fcell.2020.596069
19. Pilliod J, Moutton S, Lavie J, et al. New practical definitions for the diagnosis of autosomal recessive spastic ataxia of Charlevoix-Saguenay. Ann Neurol 2015;78(6):871–886. https://doi.org/10.1002/ana.24509
20. Riemer J, Hoepken HH, Czerwinska H, Robinson SR, Dringen R. Colorimetric ferrozine-based assay for the quantitation of iron in cultured cells. Anal Biochem 2004;331(2):370–375. https://doi.org/10.1016/j.ab.2004.03.049
21. Barbeito AG, Levade T, Delisle MB, Ghetti B, Vidal R. Abnormal iron metabolism in fibroblasts from a patient with the neurodegenerative disease hereditary ferritinopathy. Mol Neurodegener 2010;5:50. https://doi.org/10.1186/1750-1326-5-50
22. Richards S, Aziz N, Bale S, et al. Standards and guidelines for the interpretation of sequence variants: a joint consensus recommendation of the American College of Medical Genetics and Genomics and the Association for Molecular Pathology. Genet Med 2015;17(5):405–424. https://doi.org/10.1038/gim.2015.30
23. Landouré G, Zhu PP, Lourenço CM, et al. Hereditary spastic paraplegia type 43 (SPG43) is caused by mutation in C19orf12. Hum Mutat 2013;34(10):1357–1360. https://doi.org/10.1002/humu.22378
24. Di Meo I, Tiranti V. Classification and molecular pathogenesis of NBIA syndromes. Eur J Paediatr Neurol 2018;22(2):272–284. https://doi.org/10.1016/j.ejpn.2018.01.008
25. Yang Y, Zhang S, Yang W, et al. Case report: identification of a De novo C19orf12 variant in a patient with mitochondrial membrane protein-associated neurodegeneration. Front Genet 2022;13:852374. https://doi.org/10.3389/fgene.2022.852374
26. Neary D, Snowden JS, Gustafson L, et al. Frontotemporal lobar degeneration: a consensus on clinical diagnostic criteria. Neurology 1998;51(6):1546–1554. https://doi.org/10.1212/wnl.51.6.1546
27. Gambin T, Liu Q, Karolak JA, et al. Low-level parental somatic mosaic SNVs in exomes from a large cohort of trios with diverse suspected Mendelian conditions. Genet Med 2020;22(11):1768–1776. https://doi.org/10.1038/s41436-020-0897-z
28. Skowronska M, Kmiec T, Kurkowska-Jastrzębska I, Czlonkowska A. Eye of the tiger sign in a 23year patient with mitochondrial membrane protein associated neurodegeneration. J Neurol Sci 2015;352(1):110–111. https://doi.org/10.1016/j.jns.2015.03.019
29. Al Macki N, Al RI. A novel deletion mutation of exon 2 of the C19orf12 gene in an Omani family with mitochondrial membrane protein-associated neurodegeneration (MPAN). Oman Med J 2017;32(1):66–68. https://doi.org/10.5001/omj.2017.12
30. Dehghan Manshadi M, Rohani M, Rezaei A, Aryani O. A case of MPAN with "Eye of the Tiger sign," Mimicking PKAN. Mov Disord Clin Pract 2022;9(5):693–695. https://doi.org/10.1002/mdc3.13493
31. Paisán-Ruiz C, Li A, Schneider SA, et al. Widespread Lewy body and tau accumulation in childhood and adult onset dystonia-parkinsonism cases with PLA2G6 mutations. Neurobiol Aging 2012;33(4):814–823. https://doi.org/10.1016/j.neurobiolaging.2010.05.009
32. Petit F, Drecourt A, Dussiot M, et al. Defective palmitoylation of transferrin receptor triggers iron overload in Friedreich's ataxia fibroblasts. Blood 2021;2:2090–2102. https://doi.org/10.1182/blood.2020006987
33. Hinarejos I, Machuca C, Sancho P, Espinós C. Mitochondrial dysfunction, oxidative stress and neuroinflammation in neurodegeneration with brain iron accumulation (NBIA). Antioxidants 2020;9(10):1020. https://doi.org/10.3390/antiox9101020

Supporting Data

Additional Supporting Information may be found in the online version of this article at the publisher's web-site.